Electronic Supplementary Information

Intrinsic exchange bias state in silicene and germanene materials EuX_2

Dmitry V. Averyanov, Ivan S. Sokolov, Alexander N. Taldenkov, Oleg E. Parfenov, Igor A. Karateev, Oleg A. Kondratev, Andrey M. Tokmachev, Vyacheslav G. Storchak

National Research Center "Kurchatov Institute", Kurchatov Sq. 1, Moscow 123182, Russia

Experimental methods

a. Synthesis

The films of the silicene- and germanene-based materials $EuSi_2$ and $EuGe_2$ were synthesized in a Riber Compact system for molecular beam epitaxy. The substrates were Si(111) and Ge(111) wafers with a miscut angle below 0.5°. The Si substrates were high-ohmic (> 5 kOhm·cm). The natural surface oxide SiO_x was removed by heating the substrate in ultra-high vacuum ($P < 10^{-10}$ Torr) at 950 °C. GeO_x from the Ge(111) surface was removed by wet-etching in 5% NH_3(aq) with subsequent heating at 650 °C in vacuum. The substrate temperature was determined by a PhotriX ML-AAPX/090 infrared pyrometer. The synthesis of $EuSi_2$ was carried out in 2 steps. First, a layer of 4N Eu, supplied by a Knudsen cell effusion source, was deposited at room temperature on the bare surface of Si(111). The Eu pressure, $3 \cdot 10^{-8}$ Torr, was controlled by a Bayard-Alpert ionization gauge fitted at the substrate site. The film thickness was determined by the time of Eu deposition. The second step was annealing of Eu/Si(111) at 340 °C for 5 min. $EuGe_2$ was synthesized by directing Eu ($1 \cdot 10^{-8}$ Torr) at the Ge(111) substrate kept at 290 °C, followed by annealing at 500 °C for 5 min. The resulting $EuSi_2$/Si(111) and $EuGe_2$/Ge(111) films were capped with a 200 nm layer of amorphous SiO_x deposited at room temperature to ensure their protection from air.

b. Structural characterization

The atomic structure of the $EuSi_2$ and $EuGe_2$ films was established by a combination of diffraction and microscopy techniques. The state of the substrate surface during pre-treatment and the surface layer of the film were determined *in situ* employing a RHEED diffractometer furnished with the kSA 400 analytical RHEED system. X-ray diffraction patterns were produced in a Rigaku SmartLab 9 kW diffractometer operating at the Cu $K_{\alpha 1}$ wavelength. The real-space structure of $EuSi_2$ was imaged by high-resolution electron microscopy employing two types of cross-sections: $EuSi_2$/Si(111) for the side view and $EuSi_2$/$SrSi_2$/Si(001) (synthesized according to Ref. [43] of the main text) for the top view on the honeycomb structure of silicene. The cross-sections were prepared in a Helios NanoLab 600i scanning electron microscope/focused ion beam (FIB) dual beam system. The first step was capping the film with a 2 μm layer of Pt. The next step was cutting out a membrane with dimensions 2 μm × 5 μm × 5 μm by FIB milling with 30 keV Ga^+ ions. Then, the membrane was thinned with 5 keV Ga^+ ions and cleaned to reach electron transparency with 2 keV Ga^+

ions. The microstructure was determined by a TEM/STEM Cs probe corrected microscope Titan 80-300 employing the bright-field detection mode. The images were processed employing the Digital Micrograph and Tecnai Imaging and Analysis software.

c. Electron transport and magnetism

Electron transport properties of the films were studied by a Lake Shore 9709A Hall effect measurement system. Four-contact measurements of square samples with a lateral size 5 mm were employed. The electrical contacts were produced by deposition of an Ag-Sn-Ga alloy. The quality of the contacts was attested by I-V characteristic curves. Magnetic properties of the $EuSi_2$ and $EuGe_2$ films were studied by an MPMS XL-7 SQUID magnetometer. The samples were placed into plastic straws and oriented with respect to magnetic field with accuracy better than 2°; the measurements employed the reciprocating sample option. The FM moments were determined in two ways which produced close results: (i) subtraction of the diamagnetic signal of the substrate determined in a separate experiment; (ii) subtraction of contributions linear in magnetic field (see Ref. [7] of the main text).

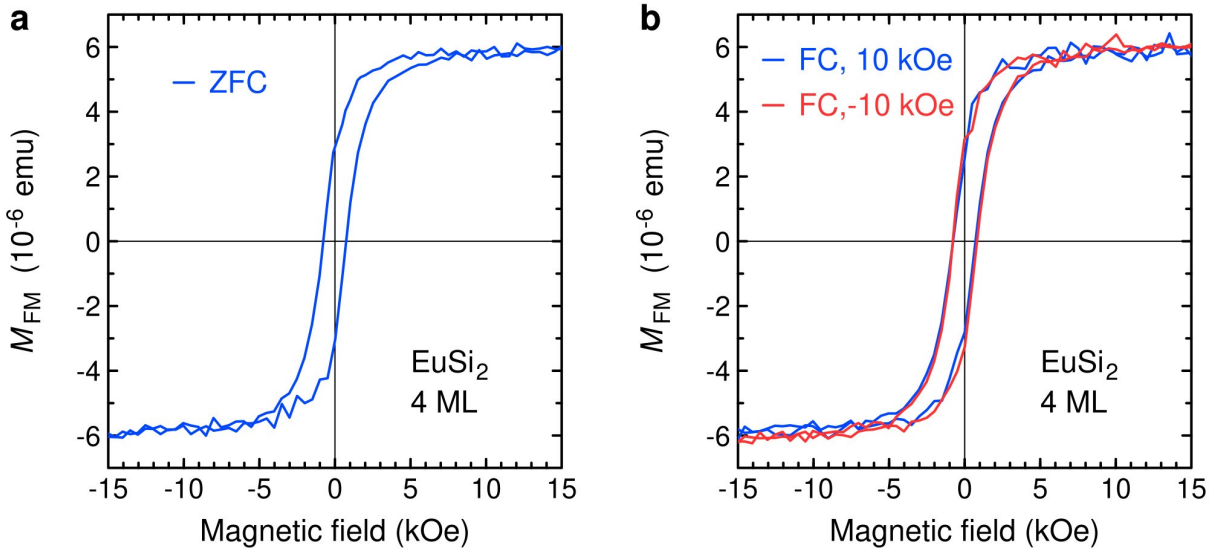

Fig. S1. Lack of exchange bias effects in 4 ML $EuSi_2$ at 2 K. a) *M-H* hysteresis loop following zero-field cooling. b) *M-H* hysteresis loops following field cooling at 10 kOe (blue) and -10 kOe (red).

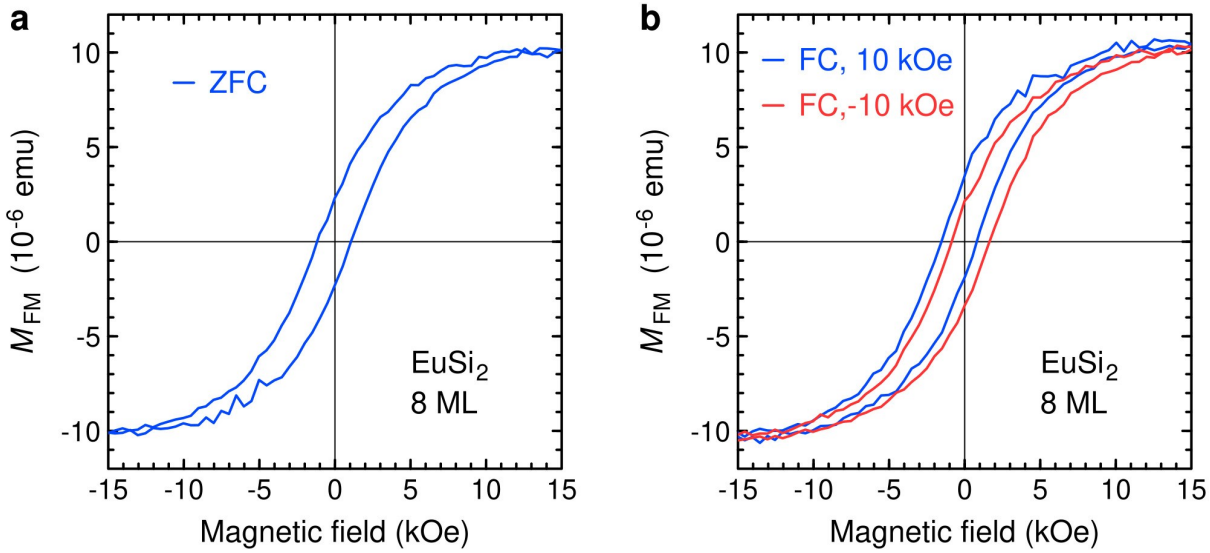

Fig. S2. Exchange bias effects in 8 ML $EuSi_2$ at 2 K. a) *M-H* hysteresis loop following zero-field cooling. b) *M-H* hysteresis loops following field cooling at 10 kOe (blue) and -10 kOe (red).

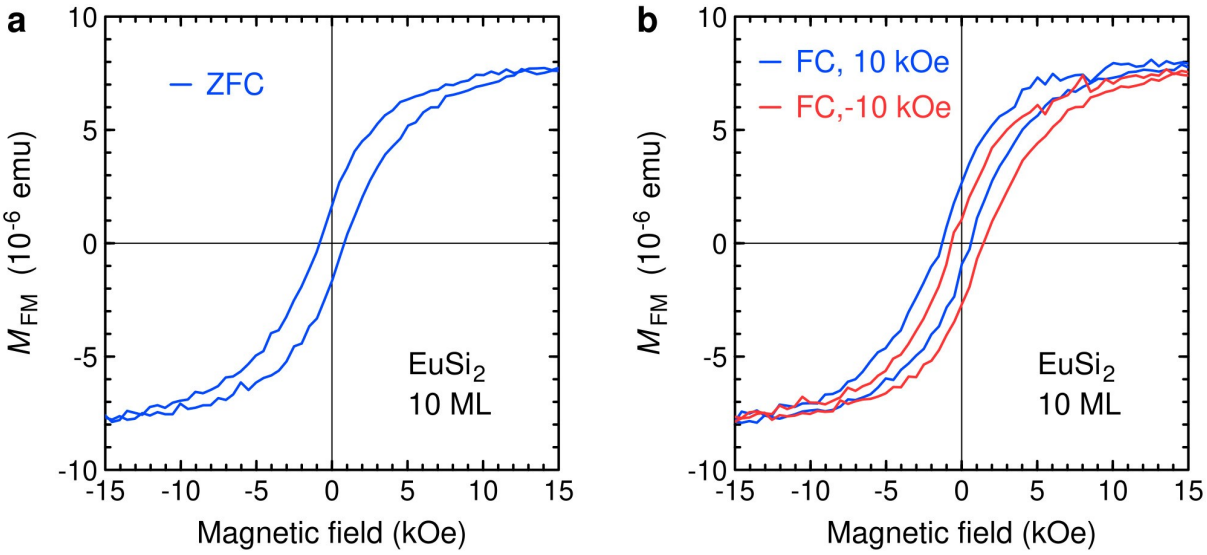

Fig. S3. Exchange bias effects in 10 ML $EuSi_2$ at 2 K. a) *M-H* hysteresis loop following zero-field cooling. b) *M-H* hysteresis loops following field cooling at 10 kOe (blue) and -10 kOe (red).